# Enhancement of subband effective mass in Ag/Ge(111) thin film quantum wells

S.-J. Tang,[1,2,*] Wen-Kai Chang,[1] Yu-Mei Chiu,[3] Hsin-Yi Chen,[1] Cheng-Maw Cheng,[2] Ku-Ding Tsuei,[2] T. Miller,[4,5] and T.-C. Chiang[4,5]

[1]*Department of Physics and Astronomy, National Tsing Hua University, Hsinchu 30013, Taiwan*

[2]*National Synchrotron Radiation Research Center, Hsinchu 30076, Taiwan*

[3]*Department of Electrophysics, National Chiao-Tung University, Hsinchu 30013, Taiwan*

[4]*Department of Physics, University of Illinois at Urbana-Champaign, 1110 West Green Street, Urbana, Illinois 61801-3080, USA*

[5]*Frederick Seitz Materials Research Laboratory, University of Illinois at Urbana-Champaign, 104 South Goodwin Avenue, Urbana, Illinois 61801-2902, USA*

(Received 29 August 2008; revised manuscript received 22 October 2008; published 8 December 2008)

Subband dispersions of quantum-well states in Ag films on Ge(111) have been determined by angle-resolved photoemission. The effective masses of the subbands at the zone center increase substantially for decreasing film thicknesses. This peculiar behavior is attributed to a kinetic constraint for standing-wave formation governed by a momentum-dependent phase-shift function. No evidence is found for in-plane electron localization within the confined geometry.

DOI: 10.1103/PhysRevB.78.245407 PACS number(s): 73.21.Fg, 68.65.Fg, 79.60.Dp

## I. INTRODUCTION

Thin films can exhibit different properties because of electron confinement and the influence of the film boundaries. These effects often lead to dramatic atomic-layer-by-atomic-layer variations in physical properties, as seen in measurements of the surface energy,[1] thermal stability,[2] work function,[3] chemisorption,[4] electron-phonon coupling,[5] superconducting transition temperature,[6–9] etc. Implications for technical applications have fostered much interest in this area of research. Electron confinement in films gives rise to discrete quantum-well states (QWS), with momentum quantized along the surface-normal direction.[10] The electronic structure is expected to remain continuous in a plane parallel to the surface, with the in-plane dispersions of the QWS largely determined by the bulk electronic structure.[11] However, Johnson *et al.*[12] found a large increase in in-plane effect masses of the QWS in Co/Cu(111) at small film thicknesses, which they attributed to a hybridization interaction between the film and the substrate. Enhanced, anomalous, and/or thickness-dependent effective masses of QWS were also reported in Ag/V(100),[13] Ag/Si(111), Ag/Si(100),[14] Cu/Co/Cu,[15] and Pb/Si(111).[16] Dil *et al.*[17] proposed lateral electron localization as an explanation for a large in-plane effective mass in Pb/Si(111), going beyond the phase accumulation model, which had been widely used to explain the QWS observed in various thin films.[18] The same proposal was made earlier by Altfeder *et al.*[19] for an explanation of their unusual results of scanning tunneling microscopy obtained from the same system.

The case of electron localization, if true, would have large impact on our general understanding of thin-film electronic structure and the utility of films in device applications. The film-substrate interface can give rise to electron scattering, especially for incommensurate systems, and Anderson-type localization can occur with a sufficiently strong scattering potential.[20] Intuitively, one possible consequence is an increased effective mass for in-plane propagation in films, which was essentially the basis for the proposal of localization, but this interpretation has remained unsubstantiated otherwise. To address this issue, we have performed a detailed investigation, by angle-resolved photoemission, of Ag films grown on Ge(111) with thicknesses in the range of 5–18 monolayers (ML). This system, with a large lattice mismatch, would be a good candidate for electron localization. Our measurements show that the effective masses increase for decreasing film thicknesses, which would seem to support the electron localization hypothesis. However, an in-depth analysis of the systematic trend reveals that the results are just as expected within the standard quantum-well model; the increased effective masses can be attributed to a kinematic constraint for standing-wave formation governed by a momentum-dependent phase-shift function. We find no evidence for electron localization in this system.

## II. EXPERIMENTAL DETAILS

In our study, angle-resolved photoemission measurements were performed at two facilities, the Synchrotron Radiation Center of the University of Wisconsin-Madison and the National Synchrotron Radiation Research Center in Taiwan; the results were consistent. A clean Ge(111)-$c(2\times8)$ surface was prepared by sputtering at a substrate temperature of 500 °C followed by annealing at 600 °C. Ag was evaporated onto the substrate maintained at 50 K. The sample was subsequently annealed at 300 K and cooled back to 50 K for the photoemission measurement. The resulting Ag films, with a bulklike lattice constant, were oriented along (111) with the crystallographic directions parallel to the same in the substrate. Atomically uniform films with exact integer monolayer thicknesses were prepared by carefully controlling the amount of deposition.[21] Photoelectron spectra were recorded as two-dimensional images with the energy and the polar emission angle as two independent variables. Dispersion relations were mapped along the $\bar{\Gamma}\bar{M}$ direction of the

 

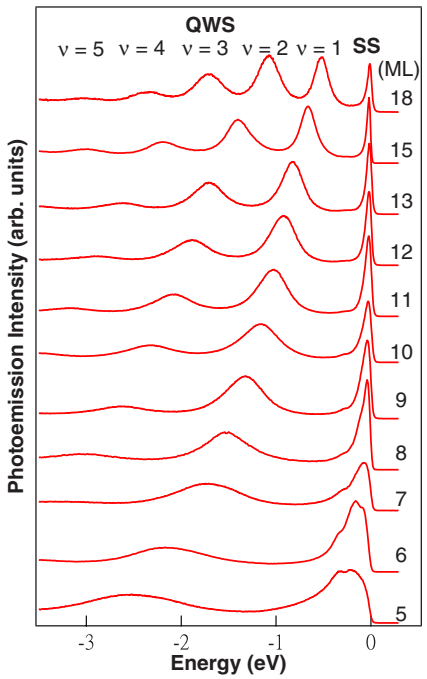


FIG. 1. (Color online) Photoemission spectra at normal emission taken from Ag films of thicknesses $N=5-18$ ML on Ge(111). SS denotes Shockley surface state. The QWS are labeled by quantum numbers $\nu=1-5$.

Ag(111) films, which is equivalent to $[11\bar{2}]$ in bulk Ag. The results to be presented herein were all taken with a photon energy of 50 eV.

## III. RESULTS AND DISCUSSION

Figure 1 shows energy distribution curves at normal emission for films ranging in thickness from 5 to 18 ML. The energy is referred to the Fermi level at $E=0$. Each QWS peak, labeled by quantum numbers $\nu=1-5$, moves toward the Fermi level as the film thickness increases. The peak labeled SS is a Shockley surface state of Ag(111). This state has a long tail, and its interaction with the substrate at small film thicknesses accounts for the complicated line shape.[22] The measured energies of the QWS at normal emission are plotted in Fig. 2. For increasing in-plane momentum (moving away from the zone center), each QWS exhibits a dispersion relation $\mathcal{E}_\nu(k_\parallel)$, where $k_\parallel$ is the wave vector parallel to the surface. The dispersion relations are governed by the Bohr-Sommerfeld quantization condition:

$$2k_\perp Nt + \phi = 2\pi n, \tag{1}$$

where $k_\perp$ is the wave vector component perpendicular to the film surface, $N$ is the film thickness in monolayers, $t$ is the monolayer thickness, and $n=N-\nu$ is a quantum number.[10] The quantity $\phi \equiv \phi(k_\perp, k_\parallel)$ is the total reflection phase shift at the two film boundaries; it depends generally on the propagation direction of the electron wave.[23,24] Solving Eq. (1) yields $k_{\nu\perp}(k_\parallel)$, the perpendicular wave vector at $k_\parallel$ for each subband.[15] This in turn yields the subband dispersion through the bulk energy dispersion relation $E(k_\perp, k_\parallel)$:

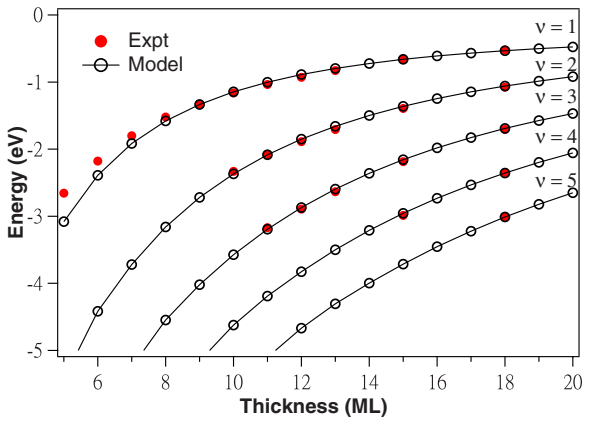


FIG. 2. (Color online) Energies of quantum-well peaks at normal emission for quantum numbers $\nu=1-5$ over the thickness range of $N=5-18$. The solid red circles are experimental results. The open circles and the curves are from a fit.

$$\mathcal{E}_\nu(k_\parallel) = E[k_{\nu\perp}(k_\parallel), k_\parallel]. \tag{2}$$

If the phase shift $\phi$ were independent of $k_\parallel$, the solution of Eq. (1) would yield a subband with a constant $k_\perp$. However, the phase-shift function is generally not this simple, and this is the source of the effective-mass variation of interest in this study.

An example of the in-plane dispersion relations $\mathcal{E}_\nu(k_\parallel)$ as mapped by angle-resolved photoemission is presented in Fig. 3 for $N=6$. The SS and the $\nu=1$ subband are indicated. The dotted curves indicate bulk band edges in Ge.[25] Both the SS and QWS dispersions are distorted near these band edges because of a hybridization interaction; this effect is most evident near the upper band edge,[16,21,22] where the states change from being fully confined to resonant. Here, we are interested in the behavior near the zone center, where in our data the states are quantum well resonances. The solid curve in Fig. 3 is a fit to the $\nu=1$ subband dispersion relation using the model function:

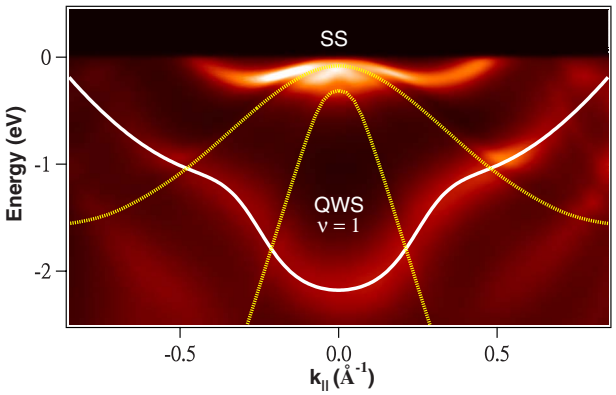


FIG. 3. (Color online) Angle-resolved photoemission data for a 6 ML film presented as a grayscale image. The vertical axis is the energy and the horizontal axis is the in-plane momentum $k_\parallel$. The SS and the $\nu=1$ subband are indicated. The dotted curves are band edges of Ge. The solid curve is fit to the $\nu=1$ subband.

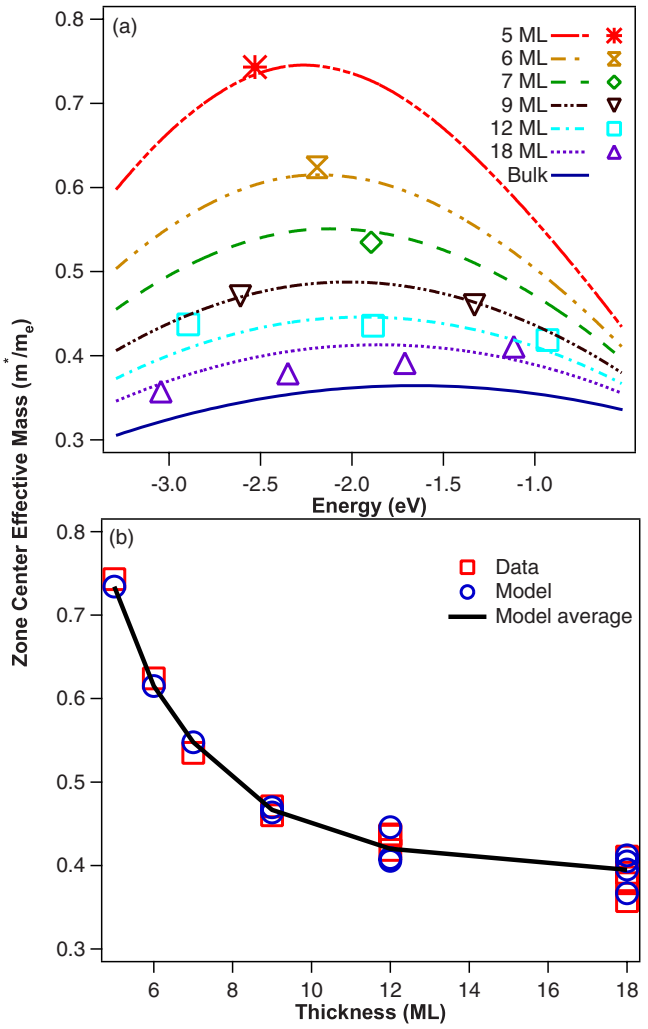


FIG. 4. (Color online) (a) Thickness and energy dependences of the zone-center subband effective mass (normalized to the free-electron mass $m_e$). The symbols are experimental results and the curves are derived from a fit. (b) The effective masses for different subbands (at different energies) are grouped together and plotted as a function of film thickness. Squares are data, circles are derived from a model fit, and the curve represents the average of the fitting results.

$$\mathcal{E}_\nu(k_\parallel) = \mathcal{E}_\nu(0) + \frac{\hbar^2 k_\parallel^2}{2m_\nu^*}\frac{1 + a_\nu k_\parallel^2 + b_\nu k_\parallel^4}{1 + c_\nu k_\parallel^2 + d_\nu k_\parallel^4}, \tag{3}$$

where a Padé function (ratio of polynomials) is employed to account for the band distortion; $a$, $b$, $c$, $d$, and the zone-center effective mass $m^*$ are treated as fitting parameters.

Values of $m^*$ extracted from the data are presented in Fig. 4(a) for $N=5-18$; data points too close to the Ge band edges for reliable extraction of $m^*$ are excluded. Apart from a dependence on energy for each thickness, $m^*$ is larger for thinner films. This thickness dependence is highlighted in Fig. 4(b), where $m^*$ for different subbands (at different energies) are grouped together for each thickness. The trend of an increasing effective mass at smaller thicknesses is evident. At first glance, this seems to suggest a hindered in-plane motion at smaller thicknesses, thus hinting at electron localization. However, as we will show, this behavior can be well explained within the standard quantum-well model; the curves in Figs. 4(a) and 4(b) and the circles in Fig. 4(b) are based on such an analysis.

The zone-center effective mass of each subband is given by:

$$\frac{1}{m_\nu^*} = \frac{1}{\hbar^2}\left.\frac{d^2\mathcal{E}_\nu(k_\parallel)}{dk_\parallel^2}\right|_{k_\parallel=0}, \tag{4}$$

which is coupled to the $k_\perp$ dependence of the band structure by Eq. (2). In turn, this is connected to the phase shift $\phi(k_\perp, k_\parallel)$ by Eq. (1). A straightforward calculation leads to

$$\frac{1}{m_\nu^*} = \frac{1}{m_{\nu 0}^*} - \frac{1}{\hbar^2}\frac{\frac{\partial E}{\partial k_\perp}\frac{\partial^2\phi}{\partial k_\parallel^2}}{2Nt + \frac{\partial\phi}{\partial k_\perp}}, \tag{5}$$

where $m_{\nu 0}^*$ is the effective mass in the bulk limit of $N\to\infty$, or

$$\frac{1}{m_{\nu 0}^*} = \frac{1}{\hbar^2}\frac{\partial^2 E(k_\perp, k_\parallel)}{\partial k_\parallel^2}. \tag{6}$$

The derivatives in Eqs. (5) and (6) are evaluated at $k_\parallel=0$. As the phase shift is a boundary property, its effect on $m^*$ is expected to diminish as $1/N$ for increasing film thicknesses. This is indeed the case as seen in Eq. (5). The extra term $\frac{\partial\phi}{\partial k_\perp}$ in the denominator is related to a charge spillage parameter discussed in earlier work (a correction term for the quantum-well width to account for the finite potential barrier height at the boundaries).[26]

To analyze the results in Figs. 2 and 4, we use an expansion of the phase-shift function to the lowest nontrivial order allowed by symmetry:

$$\phi(k_\perp, k_\parallel) = \phi_0(1 + Ak_\perp)(1 + Bk_\parallel^2), \tag{7}$$

where $\phi_0$ is a constant and $A$ and $B$ are expansion parameters. Because the $x$, $y$, and $z$ dependences of the QWS wave functions are approximately decoupled, we employ a factorized expansion form in Eq. (7). The curves in Figs. 2 and 4 are results from a simultaneous fit using Eqs. (1), (5), and (7), with the required band structure taken from an empirical analysis of Smith *et al.*[27] The fitting results describe the data well. The small discrepancies can be attributed to possible inaccuracies in the band structure and in the model phase function (just three parameters). The numerical values of the fitting parameters are $\phi_0=7.42$, $A=-0.56$ Å, and $B=3.92$ Å$^2$. Included in Fig. 4(a) is the calculated effective mass as a function of energy for $N\to\infty$ (bulk limit).

The key point of the above analysis is the predicted $1/N$ dependence of the boundary effects on the effective mass through the phase shift, as indicated by Eq. (5), which agrees well with the systematic trend seen in experiment. Thus, the enhanced effective masses at small thicknesses are well explained within the standard model. Anderson-type localization is typically a sharp transition; increasing the scattering potential causes the electronic states to become nonpropagating beyond a certain threshold. As seen in our experiment, all subbands exhibit well developed in-plane dispersion rela-

tions with a large dispersion bandwidth. This observation confirms propagating states, or the usual Bloch-type states, as characteristics of this system. Localized states would not exhibit such dispersion relations.

## IV. CONCLUSIONS

In conclusion, we have performed a detailed investigation of the subband dispersion relations in Ag films of various thicknesses deposited on Ge(111). An increased in-plane effective mass at small film thicknesses is observed. The trend follows closely a $1/N$ dependence, which can be well explained by boundary effects through a phase-shift function. There is no evidence for an abrupt onset of localization for decreasing film thicknesses.

## ACKNOWLEDGMENTS

The research of S.J.T. is supported by the National Science Council of Taiwan (Grants No. NSC 95-2120-M-007-061 and No. NSC 95-2112-M-007-062-MY3) and by the National Synchrotron Radiation Research Center. The work of T.C.C. is supported by the U.S. Department of Energy (Grant No. DE-FG02-07ER46383). T.C.C. acknowledges the Petroleum Research Fund, administered by the American Chemical Society, and the U.S. National Science Foundation (Grant No. DMR-05-03323) for partial support of the synchrotron beamline operation at the Synchrotron Radiation Center (SRC) of the University of Wisconsin-Madison. The SRC is supported by the U.S. National Science Foundation (Grant No. DMR-00-84402).

*Corresponding author. sjtang@phys.nthu.edu.tw

[1] P. Czoschke, H. Hong, L. Basile, and T.-C. Chiang, Phys. Rev. Lett. **93**, 036103 (2004); Phys. Rev. B **72**, 075402 (2005).
[2] D.-A. Luh, T. Miller, J. J. Paggel, M. Y. Chou, and T.-C. Chiang, Science **292**, 1131 (2001).
[3] J. J. Paggel, C. M. Wei, M. Y. Chou, D.-A. Luh, T. Miller, and T.-C. Chiang, Phys. Rev. B **66**, 233403 (2002).
[4] L. Aballe, A. Barinov, A. Locatelli, S. Heun, and M. Kiskinova, Phys. Rev. Lett. **93**, 196103 (2004).
[5] D.-A. Luh, T. Miller, J. J. Paggel, and T.-C. Chiang, Phys. Rev. Lett. **88**, 256802 (2002).
[6] Y. Guo, Y.-F. Zhang, X.-Y. Bao, T.-Z. Han, Z. Tang, L.-X. Zhang, W.-G. Zhu, E. G. Wang, Q. Niu, Z. Q. Qiu, J.-F. Jia, Z.-X. Zhao, and Q.-K. Xue, Science **306**, 1915 (2004).
[7] T.-C. Chiang, Science **306**, 1900 (2004).
[8] M. M. Özer, Y. Jia, Z. Zhang, J. R. Thompson, and H. H. Weitering, Science **316**, 1594 (2007).
[9] D. Eom, S. Qin, M.-Y. Chou, and C. K. Shih, Phys. Rev. Lett. **96**, 027005 (2006).
[10] T.-C. Chiang, Surf. Sci. Rep. **39**, 181 (2000).
[11] M. A. Mueller, T. Miller, and T.-C. Chiang, Phys. Rev. B **41**, 5214 (1990).
[12] P. D. Johnson, K. Garrison, Q. Dong, N. V. Smith, D. Li, J. Mattson, J. Pearson, and S. D. Bader, Phys. Rev. B **50**, 8954 (1994).
[13] T. Valla, P. Pervan, M. Milun, A. B. Hayden, and D. P. Woodruff, Phys. Rev. B **54**, 11786 (1996).
[14] I. Matsuda, T. Ohta, and H. W. Yeom, Phys. Rev. B **65**, 085327 (2002).
[15] Y. Z. Wu, C. Y. Won, E. Rotenberg, H. W. Zhao, F. Toyoma, N. V. Smith, and Z. Q. Qiu, Phys. Rev. B **66**, 245418 (2002).
[16] M. H. Upton, T. Miller, and T.-C. Chiang, Phys. Rev. B **71**, 033403 (2005).
[17] J. H. Dil, J. W. Kim, T. Kampen, K. Horn, and A. R. H. F. Ettema, Phys. Rev. B **73**, 161308(R) (2006).
[18] L. Aballe, C. Rogero, S. Gokhale, S. Kulkarni, and K. Horn, Surf. Sci. **482–485**, 488 (2001); L. Aballe, C. Rogero, and K. Horn, Phys. Rev. B **65**, 125319 (2002).
[19] I. B. Altfeder, X. Liang, T. Yamada, D. M. Chen, and V. Narayanamurti, Phys. Rev. Lett. **92**, 226404 (2004).
[20] P. W. Anderson, Phys. Rev. **109**, 1492 (1958).
[21] S.-J. Tang, L. Basile, T. Miller, and T.-C. Chiang, Phys. Rev. Lett. **93**, 216804 (2004).
[22] S.-J. Tang, T. Miller, and T.-C. Chiang, Phys. Rev. Lett. **96**, 036802 (2006).
[23] R. K. Kawakami, E. Rotenberg, E. J. Escorcia-Aparicio, H. J. Choi, J. H. Wolfe, N. V. Smith, and Z. Q. Qiu, Phys. Rev. Lett. **82**, 4098 (1999).
[24] F. G. Curti, A. Danese, and R. A. Bartynski, Phys. Rev. Lett. **80**, 2213 (1998).
[25] U. Schmid, N. E. Christensen, and M. Cardona, Phys. Rev. B **41**, 5919 (1990).
[26] P. Czoschke, H. Hong, L. Basile, and T.-C. Chiang, Phys. Rev. Lett. **91**, 226801 (2003); Phys. Rev. B **72**, 035305 (2005).
[27] N. V. Smith and L. F. Matheiss, Phys. Rev. B **9**, 1341 (1974); N. V. Smith, *ibid.* **9**, 1365 (1974).